Comptes Rendus

Physique

Xueyan Chen, Nicolas Laforge, Qingxiang Ji, Huifeng Tan, Jun Liang,
Gwenn Ulliac, Johnny Moughames, Samia Adrar, Vincent Laude
and Muamer Kadic

Introduction to mechanical metamaterials and their effective properties

Part of the Thematic Issue: Metamaterials 2
Guest editors: Boris Gralak (CNRS, Institut Fresnel, Marseille, France)
and Sébastien Guenneau (UMI2004 Abraham de Moivre, CNRS-Imperial College,
London, UK)

Metamaterials 2 / *Métamatériaux 2*

Introduction to mechanical metamaterials and their effective properties

Introduction aux métamatériaux mécaniques et à leurs propriétés effectives

Xueyan Chen[a, b]**, Nicolas Laforge**[a]**, Qingxiang Ji**[*, a, b]**, Huifeng Tan**[b]**,**
Jun Liang[b, c]**, Gwenn Ulliac**[a]**, Johnny Moughames**[a]**, Samia Adrar**[a]**,**
Vincent Laude[a] **and Muamer Kadic**[a]

[a] Institut FEMTO-ST, UMR 6174, CNRS, Université de Bourgogne Franche-Comté, 25000 Besançon, France

[b] National Key Laboratory of Science and Technology on Advanced Composites in Special Environments, Harbin Institute of Technology; 92 Xidazhi Street, Harbin, 150001, PR China

[c] Institute of Advanced Structure Technology, Beijing Institute of Technology, No. 5 South Zhongguancun Street, Haidian District, Beijing, 100081, PR China

E-mails: chenxueyan@hit.edu.cn (X. Chen), nicolas.laforge@femto-st.fr (N. Laforge), jiqingxiang@hit.edu.cn (Q. Ji), tanhf@hit.edu.cn (H. Tan), liangjun@bit.edu.cn (J. Liang), gwenn.ulliac@femto-st.fr (G. Ulliac), johnny.moughames@femto-st.fr (J. Moughames), samia.adrar@femto-st.fr (S. Adrar), vincent.laude@femto-st.fr (V. Laude), muamer.kadic@femto-st.fr (M. Kadic)

Abstract. Metamaterials are rationally designed composites made of building blocks which are composed of one or more constituent materials. Metamaterial properties can go beyond those of the ingredient materials, both qualitatively and quantitatively. In addition, their properties can be mapped on some generalized continuum model. We present the general procedure of designing elastic metamaterials based on masses and springs. We show that using this simple approach we can design any set of effective properties including linear elastic metamaterials,—defined by bulk modulus, shear modulus, mass density—and nonlinear metamaterials,—with instabilities or programmable parts. We present designs and corresponding numerical calculations to illustrate their constitutive behavior. Finally, we discuss the addition of a thermal stimulus to mechanical metamaterials.

Résumé. Les métamatériaux sont des composites de conception rationnelle constitués de briques élémentaires qui sont composées d'un ou plusieurs matériaux constitutifs. Les propriétés des métamatériaux peuvent aller au-delà de celles des matériaux constitutifs, à la fois qualitativement et quantitativement. En outre, leurs propriétés peuvent être mises en correspondance avec certains modèles de milieux continus généralisés. Nous présentons une procédure générale de conception de métamatériaux élastiques à base de

---

* Corresponding author.

systèmes de type masses et de ressorts. Nous montrons quavec cette approche simple, nous pouvons concevoir tout un ensemble de propriétés effectives, y compris celles de métamatériaux élastiques non linéaires avec instabilités ou parties programmables — définis par un module de masse, de cisaillement et une masse volumique. Nous présentons des designs et calculs numériques afin dillustrer les lois de comportement. Enfin, nous discutons de l'apport d'un stimulus thermique aux métamatériaux mécaniques.

Keywords. Metamaterials, Effective parameters, Elasticity, Anisotropy, Waves, Cauchy elasticity, Navier equation.

Mots-clés. Métamatériaux, Paramètres effectifs, Élasticité, Anisotropie, Ondes, Élasticité de Cauchy, Équation de Navier.

2020 Mathematics Subject Classification. 00-01,99-00.

1. Introduction

For the last 50 years, a huge deal of effort has been made to design novel materials by chemical synthesis (graphene [1–3], carbon nanotubes [4, 5]), by structuration (composites, fibrous materials, multilayers) [6–8], or by topology optimization in quasi-static conditions [9] or for dynamical Bloch waves (phononic crystals) [10]. The ultimate goal has been to reach an improvement in stiffness or toughness, increase or decrease in the mass density, or to absorb/reflect or transmit energy [9, 11, 12]. Indeed, in aeronautics and the automotive industry for instance, it was necessary to decrease the weight of all parts leading to a fundamental change from metals to only aluminum, alloys and composites. It is, for example, almost impossible to find a car bumper made of metal today thanks to composites (mainly fibrous). The quest for a dynamical design response (sound and vibration absorption), firstly questioned by Brillouin, was deeply expanded after pioneering works by Yablonovitch [13, 14], Monkhorst [15], and Bloch [16]. Later, the introduction of functionalities designed by transformational elastodynamics and the wish of mapping more complex media onto generalized continua motivated the expansion from Cauchy elasticity to micropolar, micromorphic or Cosserat models (an effort started in the sixties by Eringen, Maugin and other precursors [17,18]) led to the higher order gradient theories of elasticity [19] and to the modification of the Newton's second law by Willis and Milton [20].

In this paper, we revisit these innovations from the perspective of metamaterial designs taken from the literature. First, we summarize for newcomers the different models used in elasticity. Second, we focus on linear elasticity and show that using masses and spring all mechanical properties can be independently designed. Third, we present an extension of linear metamaterials toward their use for non-linear wave absorption.

2. Elasticity equations

In this section we review the complexity of the description of mechanical materials and of their constitutive laws [21].

2.1. *Hooke's spring law*

In the seventeenth century, Robert Hooke formulated the first constitutive law in mechanics that states that the force, F, needed to extend or compress a spring by a distance d is given by $F = k d$, where k is a constant (the stiffness). This law can obviously be generalized to a vectorial force $\mathbf{F}$ connecting a general vector elongation in 3D space $\mathbf{d} = (d_1, d_2, d_3)$ by a matrix of spring constants
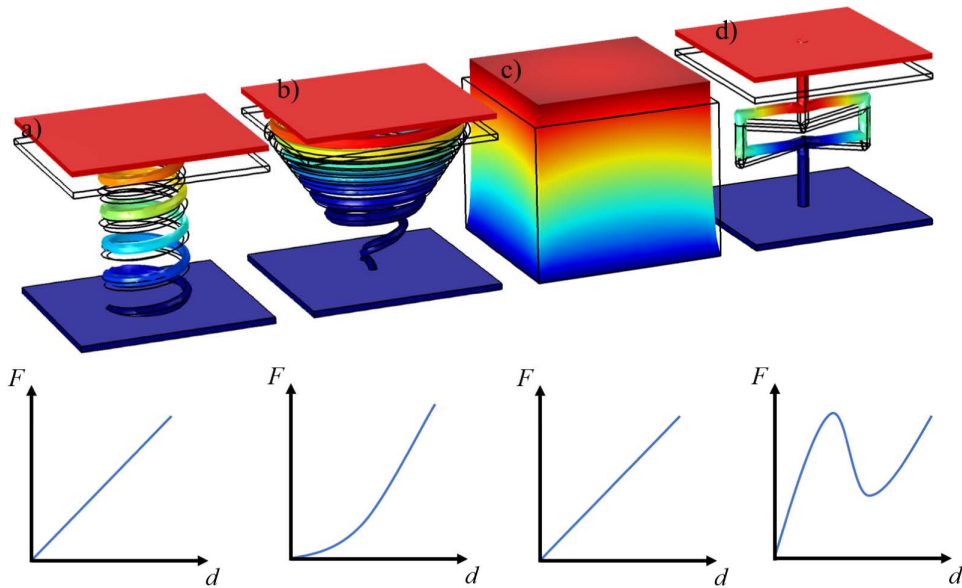
Figure 1. Under uniaxial tension, the deformations of (a) a linear spring, (b) a nonlinear spring, (c) an homogeneous cube, and (d) a geometrically nonlinear spring are depicted, respectively. The color scale measures the vertical displacement, from blue (no displacement) to red (maximum displacement). For the finite element computations, the bottom surface is clamped and a force *F* directed upward is applied at the top surface. The thin lines are for the structures at rest. Under each panel, a schematic force-elongation curve is displayed.

k as **F** = **kd**. It is well known that in the general case, the spring constant is a constant scalar (or a constant matrix), but that its magnitude can change depending on the load in a nonlinear way (either monotonically or not; see the section on nonlinear mechanics). In Figure 1 we illustrate the principles of linear and nonlinear springs and continua, a concept that we will more clearly describe later on. The scalar Hooke's law primarily relates linearly the tension of an homogeneous spring to its elongation (Figure 1(a)). If the spring is made inhomogeneous along its length, such as in Figure 1(b), then the relationship becomes nonlinear. Similarly, the homogeneous cube of Figure 1(c) can often be modelled with the linear Hooke's law, but a structural spring such as depicted in Figure 1(d) must be described using a nonlinear stiffness under large deformations. In the figure, the color scale represents the local vertical displacement with respect to the static equilibrium position under zero tension. The elongation *d* is the difference of the top displacement and the bottom displacement. Whereas in the first three cases the displacement field is basically a simple vertical gradient, in the structural spring case the displacement field varies in a more complex fashion.

Clearly, Hooke's approach can be justified only for simple spring-like geometries and for long bars. When all dimensions (pushing and lateral) of a material are comparable then this approach does not reflect properly the deformation of the body. Thus, a more general theory is required. It is called Cauchy elasticity from the contribution of Louis Cauchy to the definition of the stress tensor replacing the simple applied force by a quantity homogeneous to a force per surface area (thus with the units of pressure). Figure 2 illustrates the different components of the Cauchy stress tensor exerted on an infinitesimal cubic volume.

The stress tensor defined graphically in Figure 2 obeys the fundamental law of conservation
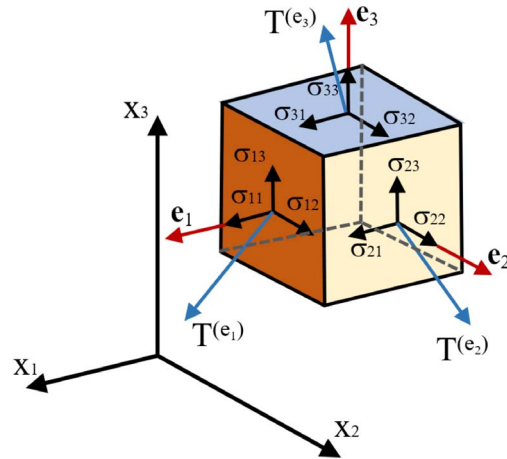
Figure 2. Illustration of the elements of the Cauchy tensor and of the orientation conven-
tion. In a Cartesian coordinate system, the stress vectors applying on each elemental plane,
$T^{(e_1)}$, $T^{(e_2)}$, and $T^{(e_3)}$ can be decomposed into a normal component and two shear compo-
nents measured along the three principal axes.

of linear momentum. Combined with the conservation of angular momentum, the stress tensor
takes a symmetric form with only six independent parameters, rather than nine, and may thus be
written:

$$
\begin{bmatrix} \sigma_{11} & \sigma_{12} & \sigma_{13} \\ \sigma_{21} & \sigma_{22} & \sigma_{23} \\ \sigma_{31} & \sigma_{32} & \sigma_{33} \end{bmatrix} = \begin{bmatrix} \sigma_1 & \sigma_6 & \sigma_5 \\ \sigma_6 & \sigma_2 & \sigma_4 \\ \sigma_5 & \sigma_4 & \sigma_3 \end{bmatrix} \tag{1}
$$

where the diagonal entries σ_1, σ_2 and σ_3 are the normal stresses, and the off-diagonal entries
$\sigma_{12} = \sigma_6$, $\sigma_{13} = \sigma_5$ and $\sigma_{23} = \sigma_4$ are the orthogonal shear stresses.

Next, the infinitesimal strain tensor for a displacement field **u** is defined by:

$$
\boldsymbol{\varepsilon} = \tfrac{1}{2}[\nabla \mathbf{u} + (\nabla \mathbf{u})^T].
$$

By construction this tensor is also symmetric. In component form, it writes as

$$
\varepsilon_{ij} = \tfrac{1}{2}(u_{i,j} + u_{j,i}), \quad i, j = 1, 2, 3,
$$

and the notation $u_{i,j} = \partial u_i / \partial x_j$. Therefore, the displacement gradient can alternatively be
expressed as

$$
\nabla \mathbf{u} = \boldsymbol{\varepsilon} + \boldsymbol{\gamma}
$$

with a skew symmetric tensor $\boldsymbol{\gamma}$ also called the rotation tensor:

$$
\boldsymbol{\gamma} = \tfrac{1}{2}[\nabla \mathbf{u} - (\nabla \mathbf{u})^T].
$$

Finally the constitutive equation between stress and stain tensors is given by the generalized
Hooke's law as

$$
\boldsymbol{\sigma} = \mathsf{C} : \boldsymbol{\varepsilon},
$$

with $\boldsymbol{\sigma}$ Cauchy's stress tensor, $\boldsymbol{\varepsilon}$ the infinitesimal strain tensor, and C a fourth-order elasticity
tensor. The latter must obey certain properties of tensors such as symmetries and positive
definiteness.

Sometimes it is difficult to model lattice metamaterials with continuum mechanics, especially
if bars get very thin and numerous. For this purpose, it is important to note that simplified
theories exist, e.g. Timoshenko's and Euler–Bernouilli beam theories. However, in the quest of an

efficient implementation they are not practical compared to finite element models. Anyway, an extensive and specific literature exists and has been used for the design of metamaterials [22–26].

2.2. *Navier's equation*

Once a rigid or deformable body is in motion, Newton's second law can be written as follows (omitting possible external forces):

$$\nabla \cdot \boldsymbol{\sigma} = \rho \, \frac{\partial^2 \mathbf{u}}{\partial t^2} \tag{2}$$

with $\boldsymbol{\rho}$ the mass density and t the time variable. If the elastic body is isotropic, then

$$\mathsf{C}_{ijkl} = \lambda \delta_{ij} \delta_{kl} + 2\mu \delta_{ij}, \tag{3}$$

where Lamé's parameters λ and μ can be expressed in terms of Poisson's ratio ν and Young's modulus E as

$$\lambda = \frac{E\nu}{(1+\nu)(1-2\nu)}, \quad \mu = \frac{E(1-\nu)}{(1+\nu)(1-2\nu)}. \tag{4}$$

In the time-harmonic regime Navier's equation at angular frequency ω is

$$\nabla \cdot \boldsymbol{\sigma} = -\rho \, \omega^2 \, \mathbf{u}. \tag{5}$$

3. Linear mechanical metamaterials

3.1. *Isotropic metamaterials*

In the isotropic case, the effective elasticity tensor that describes the elastic properties of a solid metamaterial is very simple and in fact can be decomposed in a form with only two eigenvalues (see Milton [27] and Banerjee [28]). Here, we describe how to design the most simple isotropic mechanical metamaterial (as a remark, isotropy in mechanics is not as simple as in crystallography, since space groups must be considered instead of point groups in order to describe symmetry). We start from the ideal pentamode metamaterials introduced by Milton and Cherkaev [27], as shown in Figure 3. Pentamodes are expected to avoid the coupling of compression and shear waves due to their extremely large bulk modulus, *B*, in comparison with the shear modulus, *G* [27,29]. However, it is almost impossible to fabricate such ideal pentamodes due to infinitely small connections between cones. In 2012, Kadic *et al.* realized pentamodes experimentally by modifying the diameter of thin and thick ends of double cones [29]. They investigated the effect of the overlap volume on the ratio *B/G*. They found that increasing the overlap volume stabilizes the structures, yet at the same time decreasing the ratio.

Figures 3(b) and (c) show 3D view and magnified front view electron micrographs of an optimal pentamode truss micro-lattice metamaterial fabricated by dip-in three-dimensional direct-laser-writing (DLW) optical lithography. These structures are experimentally validated to possess an extremely large *B/G* ratio which can be also observed in Figure 5(a). Figure 4 and Figure 5(b) illustrate how to independently control the bulk modulus *B* by connecting the middle part of double cones with soft loose springs. One can also fulfill the goal to control density by using parallel springs while enlarging the diameter *d*. By replacing loose springs with dense springs, it is easy to keep the bulk modulus *B* and to enhance the capacity to resist shear loading.

Actually, we can make pentamode metamaterials isotropic by adapting the optimal method presented by Buckmann *et al.* [31]. We can relate the elastic modulus, the shear modulus and Poisson's ratio to three phase velocities ν of the pentamode material, which are chosen either purely longitudinally or transversely polarized, in the *M* direction or [110] direction. We thus get
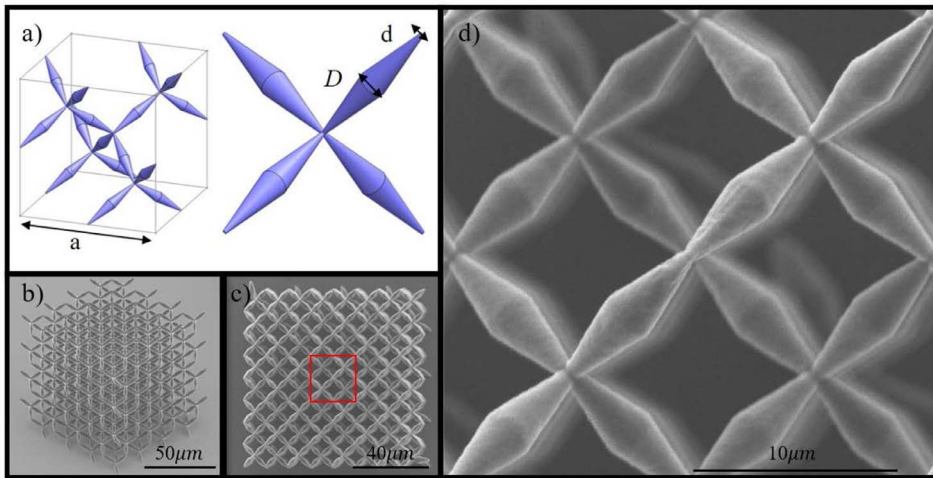
Figure 3. (a) An ideal periodic unit cell of a pentamode metamaterial with constant length a and a modified pentamode with a smaller diameter, d, at connecting parts of the double-cone strut, and a bigger diameter, D, of the middle part. 3D view (b) and magnified front view (c) electron micrograph of a pentamode truss micro-lattice metamaterial fabricated by dip-in three-dimensional direct-laser-writing (DLW) optical lithography. Front view electron micrograph (d) of an unit cell of the metamaterial part which is highlighted with a red square in (c). The samples chosen reproduce those discussed originally in Ref. [29].

a sufficient condition for isotropy as $v_{110}^L = v_{110}^{T,xy}$. This condition can be undertood as follows: the phase velocity of the longitudinal wave along the crystallographic direction [110] equals the phase velocity of the transverse wave along the same direction. The condition can be achieved by adjusting geometrical parameters or by adding additional springs. All in all, we obtain a possible way to control the 3 independent mechanical parameters and to make pentamodes isotropic by adjusting different parts of the periodic unit cell.

4. Nonlinear mechanical metamaterials

In the regime of large deformations, the stress–strain response of mechanical metamaterials [32–34] always goes through a sequence of increases [35, 36] or decreases [37, 38], and steady [39–41] or damping [42, 43] variations. Globally, the part of the graph extending beyond the initial elastic region describes the mechanical nonlinearity. Scientists usually pay much attention to the elastic region for load-bearing mechanical metamaterials [38, 43], whereas nonlinearity is important for energy absorption mechanical metamaterials [39, 43] and programmable metamaterials [11, 44]. Nonlinearity arises from two aspects, either geometrical (structural) nonlinearity or the nonlinearity of the parent materials used for building the metamaterial [45]. Geometrical nonlinearity, which is mainly determined by the topological structure and geometrical parameters, exists in systems that sustain large deformations. Geometrical structures, such as truss lattices [35, 40], shell lattices [42, 43] and plate lattices [46, 47] have to abide by two different deformation criteria: stretching dominated or bending dominated [48]. Different geometrical parameters will yield different failure modes, including stiffening or softening plastic yield [38], plastic collapse [35], linear and nonlinear buckling [39, 43], and so on. In a similar way, the mechanical properties, especially in the nonlinear region, of the parent materials also affect the failure modes
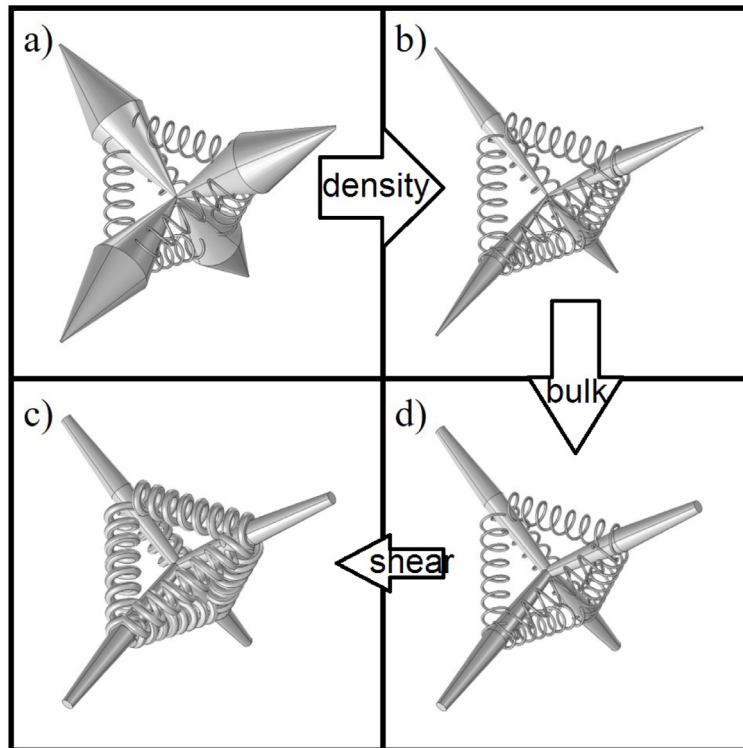
Figure 4. Illustration of optimal pentamodes with (a) a larger diameter D and additional loose springs, (b) additional loose springs, (c) a larger diameter d and additional dense springs and (d) a larger diameter d and additional loose springs.

of mechanical metamaterials. Material nonlinearity works only after the deformation of the parent materials has gone beyond the elastic region. Plastic yield will dominate the failure of most metals and polymers. However, brittle failure will be most common for ceramics, composite materials, and other ceramic-like materials. Material properties and the topological structure together with geometrical parameters decide the failure models, that is the nonlinear response, of mechanical metamaterials.

Viscous materials, for which the relationship between stress and strain depends on time, provide another possibility to design energy absorption, energy dissipation, and vibration suppression metamaterials. Their energy dissipation capacity highly depends on the angular frequency. Several mathematical models have been proposed to describe such dispersive relationships. The Maxwell loss model [49, 50] is probably the oldest viscoelastic model and can be represented by a purely viscous damper and a purely elastic spring connected in series, as shown in Figure 6(a). The dynamic modulus $E^*(\omega) = E' + iE''$ is obtained following the rules for admittance in equivalent circuits. In the case of the Maxwell model,

$$\frac{1}{E^*} = \frac{1}{E} + \frac{1}{i\omega\eta} \tag{6}$$

which yields

$$E' = \frac{\tau^2\omega^2}{\tau^2\omega^2 + 1}E, \quad E'' = \frac{\tau\omega}{\tau^2\omega^2 + 1}E, \tag{7}$$
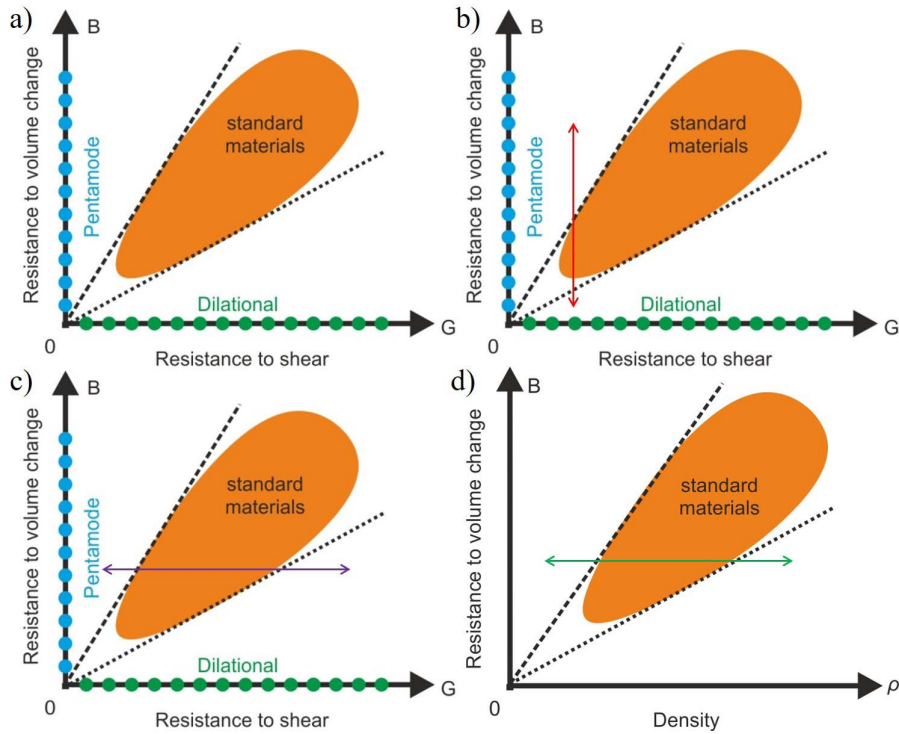
Figure 5. Milton's maps of (a) pentamode metamaterials and (b), (c) optimal pentamode metamaterials with different geometrical parameters. Ashby's map (d) of optimal pentamode metamaterials. This figure is inspired by Ref. [30].

with $\tau = \eta/E$. If we connect elastic and viscous elements in parallel, as in Figure 6(b), we get the generalized Kelvin–Voigt model [49, 50]

$$E^* = E + i\omega\eta. \tag{8}$$

Then obviously $E' = E$ and $E'' = \omega\eta$. Combining a serial Maxwell branch in parallel with a purely elastic branch, the more realistic model of the standard linear solid is obtained, as depicted in Figure 6(c). The model contains two independent elastic elements, E_1 and E_2, and a viscous element η, and is also known as the Zener model [49–51]. The complex dynamic modulus is

$$E^*(\omega) = \left(\frac{1}{E_1} + \frac{1}{i\omega\eta} \right)^{-1} + E_2, \tag{9}$$

leading to

$$E'(\omega) = \frac{\tau^2\omega^2}{\tau^2\omega^2 + 1} E_1 + E_2, \tag{10}$$

$$E''(\omega) = \frac{\tau\omega}{\tau^2\omega^2 + 1} E_1. \tag{11}$$

Figure 6 depicts the three previous elastic-viscous models and the corresponding relationships between dynamics modulus and vibration frequency. The equations are simple enough but often prove insufficient. For instance, the Maxwell model successfully captures the evolution of the imaginary dynamic modulus as a function of vibration frequency, but fails to describe the dependence of the real part on frequency. It should be noted that any solid material must have a non zero elastic modulus in the absence of vibrations, i.e. at the zero frequency. Hence, the
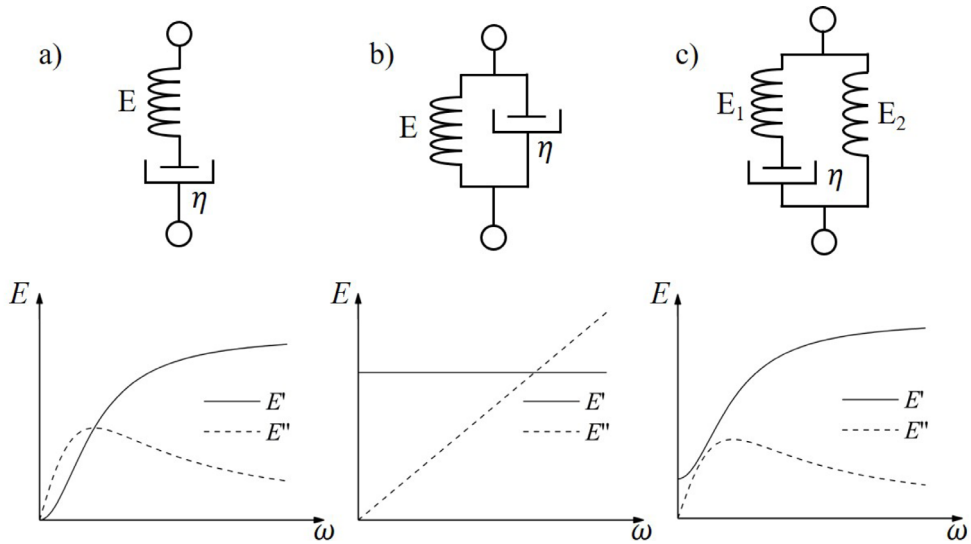
Figure 6. (a) Maxwell, (b) Voigt and (c) the standard linear solid simplified elastic-viscous models are depicted in analogy with equivalent electrical circuits. Young's modulus E is analogous to a real-valued admittance, whereas viscosity contributes a $i\omega\eta$ admittance similar to a capacitance. The resulting relationship between dynamic modulus and angular frequency is depicted below each equivalent circuit model (see text for their expressions).

Maxwell loss model is not physical in the limit of low frequencies. Finally, the Kelvin–Voigt model is too ideal to describe nonlinear variations of the dynamic modulus.

4.1. *Tailoring the stress–strain curve*

A central issue of mechanical metamaterial design is indeed to tailor the stress–strain curve to follow given shapes chosen in order to meet given requirements [35, 39, 46]. As outlined in the previous section, the geometrical structure is one of most important factors in metamaterial design. Here, we will give three examples to illustrate how to tailor the stress–strain curve by optimizing the structure.

Let us start from a conventional spring which is the most basic elastic element in a mechanical metamaterial. When a conventional spring is compressed or stretched from its rest position (strained), a stress distribution appears along the length. Figure 1(a) illustrates the force versus elongation curve. The spring constant is almost a constant as long as deformation does not go beyond spring stoke. Under certain circumstances, however, a spring constant increasing with applied strain is needed. In this case, replacing the constant spacing spring coils with graded spacing spring coils, or replacing the constant major radius with an increasing major radius, a progressive rate spring can be obtained, as Figure 1(b) depicts.

Second, the simple cubic solid structure, that is a base element in 3D mechanical metamaterials, can be used to implement any geometrical structure by periodic repetition of a unit cell. Figure 1(c) shows the deformation and the corresponding stress–strain curve of an homogeneous cubic unit cell under tension. Clearly, Poisson's ratio is positive and a conventional elastic–plastic tensile response is obtained. However, the structure [32] shown in Figure 1(d), which is composed of several relatively small simple cubic elements, has a totally different deformation behavior: it
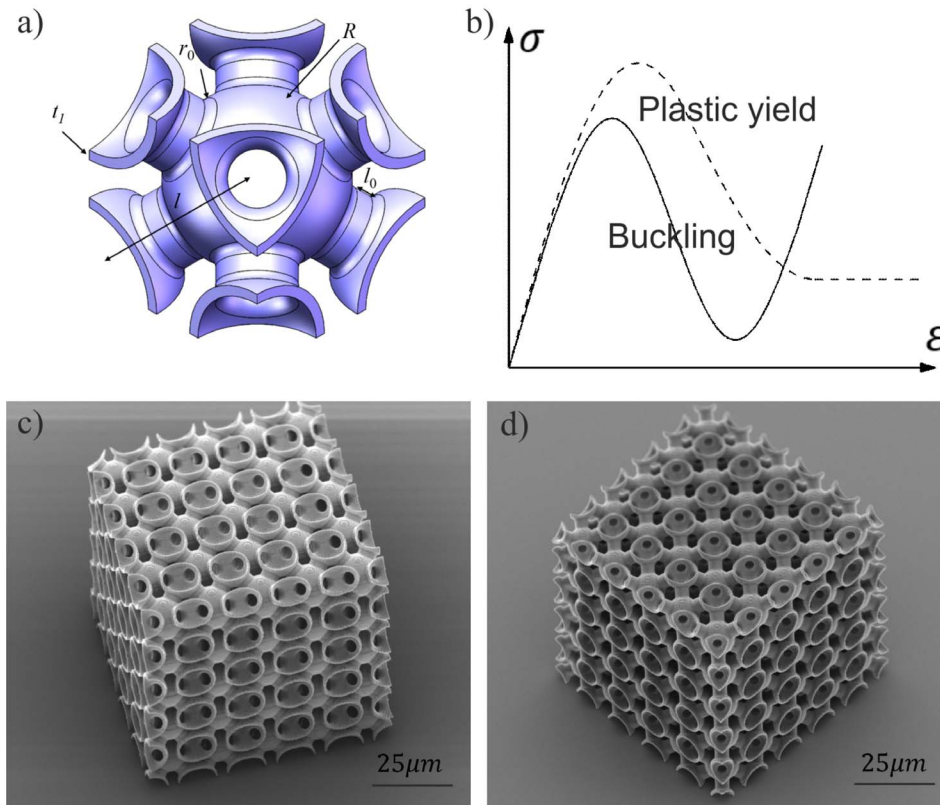
Figure 7. Body centered cubic (BCC) shell-lattice metamaterial. (a) A unit cell is depicted along with its geometrical parameters. (b) Two different failure models can be observed for the shell-lattice material, either plastic yield or buckling. The optimal designs obtained for (c) energy absorption and (d) bearing load were fabricated by two-photon lithography.

is auxetic (Poisson's ratio is negative). Moreover, the failure mode changes from elastic–plastic to plastic bending. Note that such mechanical behavior is unusual in natural materials.

Third, we consider the control of the failure mode of mechanical metamaterials. The body centered cubic (BCC) shell-lattice metamaterial depicted in Figure 7 has high stiffness, high strength, and large specific energy absorption at low relative density [52]. The compressive failure mode of the metamaterial, either dominated by plastic yield or buckling, is affected by the geometrical parameters defining the structure, including the spherical node radius R, the cylindrical strut radius r, the smooth connecting shell radius r_0, the cylindrical strut length l_0, the total length l, and thickness t_1. These geometrical parameters are not independent: we have $r_0 = 2R - r$ and $l = l_0 + 2\sqrt{3}(R - r)$. Further fixing the total length of the shell strut and setting the relative density to 0.05, only two independent parameters are left, for instance the spherical node radius R and the smooth connecting shell radius r_0. After topology optimization, we obtained two different functional shell metamaterials: a buckling dominated metamaterial ($R/r = 2.3$ and $l_0/(l - l_0) = 0.1$) and a yield dominated metamaterial ($R/r = 2.5$ and $l_0/(l - l_0) = 0.2$). The buckling dominated metamaterial can almost recover 92% of its original shape after compressions in excess of 60% strain, which makes it a good candidate for energy absorption. The yield dominated metamaterial has higher stiffness, higher strength and better load bearing capacity. These examples encourage one to make possible the impossible.

4.2. *Material nonlinearities and their use for energy absorption*

Nonlinear metamaterials are widely used in our daily life for energy absorption [53–56]. Aiming at absorbing as much energy as possible, nonlinear metamaterials were usually designed to obtain a relatively large peak force with large deformation [35, 55, 57]. Most metamaterials utilize plastic deformation or brittle fracture of micro-struts [37], shell [43] or plate [46, 47] to dissipate a large amount of energy. Stretching dominated metamaterials [43, 46, 47], which are maybe the most famous plastic yield metamaterials, have been proven to possess extraordinary loading bear capacity and energy absorption at high relative density. In contrast, bending dominated metamaterials [35, 41], which make use of plastic bending joint, allow for large deformation and provide relatively large and nearly constant stress area in the nonlinear region at low relative density. In addition, reusable energy metamaterials [39, 58, 59] were proposed to extend their life span. By utilizing elastic buckling of shell, straight strut and curved beam, reusable energy metamaterials were shown to present unusual features including mechanical multi-stability [60, 61], close to 100 percent recovery after unloading [39, 55, 58], and controllable mechanical response [44].

5. Thermomechanical metamaterials

Systems placed in a thermal environment are sensitive to temperature changes of their surroundings. An ambient temperature change ΔT will cause a thermal strain $\alpha_{ij}\Delta T$ in an elastic solid due to thermal expansion. Generally, thermal expansion is described by a symmetric tensor of rank two

$$\alpha_{ij} = \begin{bmatrix} \alpha_{11} & \alpha_{12} & \alpha_{13} \\ \alpha_{12} & \alpha_{22} & \alpha_{23} \\ \alpha_{13} & \alpha_{23} & \alpha_{33} \end{bmatrix}. \tag{12}$$

For isotropic solids, the thermal expansion tensor is proportional to the identity matrix, $\alpha_{ij} = \alpha \boldsymbol{I}$, where $\boldsymbol{I}$ is the rank-two identity matrix and α is the thermal length expansion defined by

$$\alpha = \frac{1}{L}\frac{\partial L}{\partial T}. \tag{13}$$

In the elastic stress–strain relation, thermal strain has to be subtracted from total strain, leading to the relation

$$\sigma_{ij} = C_{ijkl}(\varepsilon_{kl} - \alpha_{kl}\Delta T) \tag{14}$$

or, in the case of isotropic solids,

$$\sigma_{ij} = 2\mu\varepsilon_{ij} + \lambda\varepsilon_{ij}\delta_{ij} - (2\mu + 3\lambda)\alpha\Delta T\delta_{ij}. \tag{15}$$

Note that the temperature dependence of the elastic constants was neglected in the above equations.

Temperature variations can result both in thermal expansion and in geometry changes, which can be problematic in temperature-sensitive applications that require thermal stability like space frame trusses, satellite antennas and space crafts [62, 63]. Alternatively, thermal expansion can also be tailored to achieve some required thermal deformation and behavior. Material systems and structures can be deliberately designed to deform in a controllable manner in response to a temperature stimulus. Applications based on this principle include morphing structures [64], large reversible shape changing components [65], micro-actuators [66], self-assembly systems [67], grippers for soft micro-robotics [68], biology devices [69], and so on.

Generally, those applications bring in demands on controllable coefficients of thermal expansion (CTE), e.g. large, positive, negative or zero thermal expansion materials and structures. Many efforts have been made to create architectured materials with tunable CTE using two constituents

with widely different thermal expansion combined in space. Different concepts were proposed under this approach and each has its working principle and specific advantages. One major concept is utilizing the bending-dominated bi-material strip, based on which some researchers proposed cellular solid structures with unbounded thermal expansion [70, 71]. Other concepts include stretch-dominated structures composed of nested double-parallel units with large stiffness [71], flexure blade structures with high CTE tunability [72], and tetrahedron structure combined with sizable CTE tunability and large stiffness [73, 74]. Another major approach is to generate CTE tunability via topology optimization [75–77]. Structures obtained following this method are generally more complicated. Finally, using 3D printing technologies, researchers have managed to directly print metamaterials with controllable thermal expansion and have achieved rather high but negative thermal expansion coefficients [72, 78, 79].

6. Conclusion

In this paper, we have presented general procedures to design mechanical metamaterials in both the linear and the nonlinear regimes using an effective medium approach based on simple mechanical models. We have emphasized the complexity and the opportunities in the nonlinear case if one uses viscosity or plasticity. Finally, we have summarized proposals aiming at using an external stimulus (variation of temperature) to change the shape of designed metamaterials.

Acknowledgments

References

[1] M. J. Allen, V. C. Tung, R. B. Kaner, "Honeycomb carbon: a review of graphene", *Chem. Rev.* **110** (2009), no. 1, p. 132-145.

[2] Y. Shao, J. Wang, H. Wu, J. Liu, I. A. Aksay, Y. Lin, "Graphene based electrochemical sensors and biosensors: a review", *Electroanalysis* **22** (2010), no. 10, p. 1027-1036.

[3] M. Yi, Z. Shen, "A review on mechanical exfoliation for the scalable production of graphene", *J. Mater. Chem. A* **3** (2015), no. 22, p. 11700-11715.

[4] G. Mittal, V. Dhand, K. Y. Rhee, S.-J. Park, W. R. Lee, "A review on carbon nanotubes and graphene as fillers in reinforced polymer nanocomposites", *J. Ind. Eng. Chem.* **21** (2015), p. 11-25.

[5] A. D. Moghadam, E. Omrani, P. L. Menezes, P. K. Rohatgi, "Mechanical and tribological properties of self-lubricating metal matrix nanocomposites reinforced by carbon nanotubes (CNTs) and graphene–a review", *Composites B* **77** (2015), p. 402-420.

[6] J. J. Carruthers, A. Kettle, A. Robinson, "Energy absorption capability and crashworthiness of composite material structures: a review", *Appl. Mech. Rev.* **51** (1998), no. 10, p. 635-649.

[7] D. Liu, Y. Tang, W. Cong, "A review of mechanical drilling for composite laminates", *Compos. Struct.* **94** (2012), no. 4, p. 1265-1279.

[8] R. F. Gibson, "A review of recent research on mechanics of multifunctional composite materials and structures", *Compos. Struct.* **92** (2010), no. 12, p. 2793-2810.

[9] X. Yu, J. Zhou, H. Liang, Z. Jiang, L. Wu, "Mechanical metamaterials associated with stiffness, rigidity and compressibility: A brief review", *Prog. Mater. Sci.* **94** (2018), p. 114-173.

[10] A. Srivastava, "Elastic metamaterials and dynamic homogenization: a review", *Int. J. Smart Nano Mater.* **6** (2015), no. 1, p. 41-60.

[11] K. Bertoldi, V. Vitelli, J. Christensen, M. van Hecke, "Flexible mechanical metamaterials", *Nat. Rev. Mater.* **2** (2017), no. 11, p. 17066.

[12] J.-H. Lee, J. P. Singer, E. L. Thomas, "Micro-/nanostructured mechanical metamaterials", *Adv. Mater.* **24** (2012), no. 36, p. 4782-4810.

[13] E. Yablonovitch, "Photonic band-gap structures", *J. Opt. Soc. Am. B* **10** (1993), no. 2, p. 283-295.

[14] E. Yablonovitch, T. Gmitter, K.-M. Leung, "Photonic band structure: The face-centered-cubic case employing nonspherical atoms", *Phys. Rev. Lett.* **67** (1991), no. 17, p. 2295.

[15] H. J. Monkhorst, J. D. Pack, "Special points for Brillouin-zone integrations", *Phys. Rev. B* **13** (1976), no. 12, p. 5188.

[16] P. E. Blöchl, O. Jepsen, O. K. Andersen, "Improved tetrahedron method for Brillouin-zone integrations", *Phys. Rev. B* **49** (1994), no. 23, p. 16223.

[17] A. C. Eringen, E. S. Suhubi, S. Cowin, "Elastodynamics (volume 1, finite motions)", *J. Appl. Mech.* **42** (1975), p. 748.

[18] G. A. Maugin, "Applications of an energy-momentum tensor in nonlinear elastodynamics: Pseudomomentum and eshelby stress in solitonic elastic systems", *J. Mech. Phys. Solids* **40** (1992), no. 7, p. 1543-1558.

[19] J. Achenbach, *Wave Propagation in Elastic Solids, Vol. 16*, Elsevier, Amsterdam, The Netherlands, 2012.

[20] G. W. Milton, J. R. Willis, "On modifications of Newton's second law and linear continuum elastodynamics", *Proc. R. Soc. A* **463** (2007), no. 2079, p. 855-880.

[21] M. Kadic, G. W. Milton, M. van Hecke, M. Wegener, "3D metamaterials", *Nat. Rev. Phys.* **1** (2019), no. 3, p. 198-210.

[22] P. Martinsson, A. Movchan, "Vibrations of lattice structures and phononic band gaps", *Q. J. Mech. Appl. Math.* **56** (2003), no. 1, p. 45-64.

[23] D. Colquitt, I. Jones, N. Movchan, A. Movchan, "Dispersion and localization of elastic waves in materials with microstructure", *Proc. R. Soc. A* **467** (2011), no. 2134, p. 2874-2895.

[24] A. Piccolroaz, A. Movchan, "Dispersion and localisation in structured Rayleigh beams", *Int. J. Solids Struct.* **51** (2014), no. 25-26, p. 4452-4461.

[25] A. N. Norris, "Low-frequency dispersion and attenuation in partially saturated rocks", *J. Acoust. Soc. Am.* **94** (1993), no. 1, p. 359-370.

[26] C. Findeisen, J. Hohe, M. Kadic, P. Gumbsch, "Characteristics of mechanical metamaterials based on buckling elements", *J. Mech. Phys. Solids* **102** (2017), p. 151-164.

[27] G. W. Milton, A. V. Cherkaev, "Which elasticity tensors are realizable?", *J. Eng. Mater. Technol.* **117** (1995), no. 4, p. 483-493.

[28] B. Banerjee, *An Introduction to Metamaterials and Waves in Composites*, CRC Press, Boca Raton, Florida, USA, 2011.

[29] M. Kadic, T. Bückmann, N. Stenger, M. Thiel, M. Wegener, "On the practicability of pentamode mechanical metamaterials", *Appl. Phys. Lett.* **100** (2012), no. 19, article no. 191901.

[30] M. Kadic, T. Bückmann, R. Schittny, M. Wegener, "Metamaterials beyond electromagnetism", *Rep. Prog. Phys.* **76** (2013), no. 12, article no. 126501.

[31] T. Bückmann, R. Schittny, M. Thiel, M. Kadic, G. W. Milton, M. Wegener, "On three-dimensional dilational elastic metamaterials", *New J. Phys.* **16** (2014), no. 3, article no. 033032.

[32] T. Bückmann, N. Stenger, M. Kadic, J. Kaschke, A. Frölich, T. Kennerknecht, C. Eberl, M. Thiel, M. Wegener, "Tailored 3D mechanical metamaterials made by dip-in direct-laser-writing optical lithography", *Adv. Mater.* **24** (2012), no. 20, p. 2710-2714.

[33] T. Frenzel, M. Kadic, M. Wegener, "Three-dimensional mechanical metamaterials with a twist", *Science* **358** (2017), no. 6366, p. 1072-1074.

[34] I. Fernandez-Corbaton, C. Rockstuhl, P. Ziemke, P. Gumbsch, A. Albiez, R. Schwaiger, T. Frenzel, M. Kadic, M. Wegener, "New twists of 3D chiral metamaterials", *Adv. Mater.* **31** (2019), no. 26, article no. 1807742.

[35] R. Gümrük, R. Mines, "Compressive behaviour of stainless steel micro-lattice structures", *Int. J. Mech. Sci.* **68** (2013), p. 125-139.

[36] T. Tancogne-Dejean, D. Mohr, "Elastically-isotropic truss lattice materials of reduced plastic anisotropy", *Int. J. Solids Struct.* **138** (2018), p. 24-39.

[37] T. Tancogne-Dejean, D. Mohr, "Stiffness and specific energy absorption of additively-manufactured metallic bcc metamaterials composed of tapered beams", *Int. J. Mech. Sci.* **141** (2018), p. 101-116.

[38] V. S. Deshpande, N. A. Fleck, M. F. Ashby, "Effective properties of the octet-truss lattice material", *J. Mech. Phys. Solids* **49** (2001), no. 8, p. 1747-1769.

[39] T. Frenzel, C. Findeisen, M. Kadic, P. Gumbsch, M. Wegener, "Tailored buckling microlattices as reusable light-weight shock absorbers", *Adv. Mater.* **28** (2016), no. 28, p. 5865-5870.

[40] T. Tancogne-Dejean, A. B. Spierings, D. Mohr, "Additively-manufactured metallic micro-lattice materials for high specific energy absorption under static and dynamic loading", *Acta Mater.* **116** (2016), p. 14-28.

[41] X. Cao, S. Duan, J. Liang, W. Wen, D. Fang, "Mechanical properties of an improved 3D-printed rhombic dodecahedron stainless steel lattice structure of variable cross section", *Int. J. Mech. Sci.* **145** (2018), p. 53-63.

[42] S. C. Han, J. W. Lee, K. Kang, "A new type of low density material: Shellular", *Adv. Mater.* **27** (2015), no. 37, p. 5506-5511.

[43] C. Bonatti, D. Mohr, "Smooth-shell metamaterials of cubic symmetry: Anisotropic elasticity, yield strength and specific energy absorption", *Acta Mater.* **164** (2019), p. 301-321.

[44] B. Florijn, C. Coulais, M. van Hecke, "Programmable mechanical metamaterials", *Phys. Rev. Lett.* **113** (2014), no. 17, article no. 175503.

[45] L. J. Gibson, M. F. Ashby, *Cellular Solids: Structure and Properties*, Cambridge University Press, Cambridge, UK, 1999.

[46] T. Tancogne-Dejean, M. Diamantopoulou, M. B. Gorji, C. Bonatti, D. Mohr, "3D plate-lattices: An emerging class of low-density metamaterial exhibiting optimal isotropic stiffness", *Adv. Mater.* **30** (2018), no. 45, article no. 1803334.

[47] J. Berger, H. Wadley, R. McMeeking, "Mechanical metamaterials at the theoretical limit of isotropic elastic stiffness", *Nature* **543** (2017), no. 7646, p. 533.

[48] V. Deshpande, M. Ashby, N. Fleck, "Foam topology: bending versus stretching dominated architectures", *Acta Mater.* **49** (2001), no. 6, p. 1035-1040.

[49] R. S. Lakes, *Viscoelastic Solids, Vol. 9*, CRC Press, Boca Raton, Florida, USA, 1998.

[50] R. Christensen, *Theory of Viscoelasticity: An Introduction*, Academic Press Inc., New York, USA, 2012.

[51] C. M. Zener, S. Siegel, "Elasticity and anelasticity of metals", *J. Phys. Chem.* **53** (1949), no. 9, p. 1468-1468.

[52] X. Chen, Q. Ji, J. Wei, H. Tan, J. Yu, P. Zhang, V. Laude, M. Kadic, "Light-weight shell-lattice metamaterials for mechanical shock absorption", *Int. J. Mech. Sci.* **169** (2020), article no. 105288.

[53] G. Lu, T. Yu, *Energy Absorption of Structures and Materials*, Woodhead Publishing Limited, Cambridge, UK, 2003.

[54] L. Salari-Sharif, T. A. Schaedler, L. Valdevit, "Energy dissipation mechanisms in hollow metallic microlattices", *J. Mater. Res.* **29** (2014), no. 16, p. 1755-1770.

[55] L. R. Meza, S. Das, J. R. Greer, "Strong, lightweight, and recoverable three-dimensional ceramic nanolattices", *Science* **345** (2014), no. 6202, p. 1322-1326.

[56] J. Ma, Z. You, "Energy absorption of thin-walled square tubes with a prefolded origami pattern part I: geometry and numerical simulation", *J. Appl. Mech.* **81** (2014), no. 1, article no. 011003.

[57] S. Li, H. Fang, S. Sadeghi, P. Bhovad, K.-W. Wang, "Architected origami materials: How folding creates sophisticated mechanical properties", *Adv. Mater.* **31** (2019), no. 5, article no. 1805282.

[58] T. A. Schaedler, A. J. Jacobsen, A. Torrents, A. E. Sorensen, J. Lian, J. R. Greer, L. Valdevit, W. B. Carter, "Ultralight metallic microlattices", *Science* **334** (2011), no. 6058, p. 962-965.

[59] J. L. Silverberg, A. A. Evans, L. McLeod, R. C. Hayward, T. Hull, C. D. Santangelo, I. Cohen, "Using origami design principles to fold reprogrammable mechanical metamaterials", *Science* **345** (2014), no. 6197, p. 647-650.

[60] S. Shan, S. H. Kang, J. R. Raney, P. Wang, L. Fang, F. Candido, J. A. Lewis, K. Bertoldi, "Multistable architected materials for trapping elastic strain energy", *Adv. Mater.* **27** (2015), no. 29, p. 4296-4301.

[61] K. Bertoldi, "Harnessing instabilities to design tunable architected cellular materials", *Annu. Rev. Mater. Res.* **47** (2017), p. 51-61.

[62] T.-C. Lim, "Negative thermal expansion in transversely isotropic space frame trusses", *Phys. Status Solidi B* **250** (2013), no. 10, p. 2062-2069.

[63] D. G. Gilmore, *Spacecraft Thermal Control Handbook*, Fundamental Technologies, vol. 1, American Institute of Aeronautics and Astronautics, Reston, Virginia, USA, 2002, Online version available at: http://www.knovel.com/knovel2/Toc.jsp, 373-403 pages.

[64] Q. Zhang, J. Wommer, C. ORourke, J. Teitelman, Y. Tang, J. Robison, G. Lin, J. Yin, "Origami and kirigami inspired self-folding for programming three-dimensional shape shifting of polymer sheets with light", *Extreme Mech. Lett.* **11** (2017), p. 111-120.

[65] Y. Mao, Z. Ding, C. Yuan, S. Ai, M. Isakov, J. Wu, T. Wang, M. L. Dunn, H. J. Qi, "3D printed reversible shape changing components with stimuli responsive materials", *Sci. Rep.* **6** (2016), p. 24761.

[66] J. B. Hopkins, K. J. Lange, C. M. Spadaccini, "Designing microstructural architectures with thermally actuated properties using freedom, actuation, and constraint topologies", *J. Mech. Design* **135** (2013), no. 6, article no. 061004.

[67] S. Tibbits, "Design to self-assembly", *Archit. Design* **82** (2012), no. 2, p. 68-73.

[68] J. C. Breger, C. Yoon, R. Xiao, H. R. Kwag, M. O. Wang, J. P. Fisher, T. D. Nguyen, D. H. Gracias, "Self-folding thermo-magnetically responsive soft microgrippers", *ACS Appl. Mater. Interfaces* **7** (2015), no. 5, p. 3398-3405.

[69] G. Stoychev, N. Puretskiy, L. Ionov, "Self-folding all-polymer thermoresponsive microcapsules", *Soft Matter* **7** (2011), no. 7, p. 3277-3279.

[70] R. Lakes, "Dense solid microstructures with unbounded thermal expansion", *J. Mech. Behav. Mater.* **7** (1996), no. 2, p. 85-92.

[71] J. Lehman, R. S. Lakes, "Stiff, strong, zero thermal expansion lattices via material hierarchy", *Compos. Struct.* **107** (2014), p. 654-663.

[72] Q. Wang, J. A. Jackson, Q. Ge, J. B. Hopkins, C. M. Spadaccini, N. X. Fang, "Lightweight mechanical metamaterials with tunable negative thermal expansion", *Phys. Rev. Lett.* **117** (2016), no. 17, article no. 175901.

[73] C. A. Steeves, S. L. d. S. e Lucato, M. He, E. Antinucci, J. W. Hutchinson, A. G. Evans, "Concepts for structurally robust materials that combine low thermal expansion with high stiffness", *J. Mech. Phys. Solids* **55** (2007), no. 9, p. 1803-1822.

[74] G. Jefferson, T. A. Parthasarathy, R. J. Kerans, "Tailorable thermal expansion hybrid structures", *Int. J. Solids Struct.* **46** (2009), no. 11-12, p. 2372-2387.

[75] O. Sigmund, S. Torquato, "Composites with extremal thermal expansion coefficients", *Appl. Phys. Lett.* **69** (1996), no. 21, p. 3203-3205.

[76] O. Sigmund, S. Torquato, "Design of materials with extreme thermal expansion using a three-phase topology optimization method", *J. Mech. Phys. Solids* **45** (1997), no. 6, p. 1037-1067.

[77] S. Watts, D. A. Tortorelli, "Optimality of thermal expansion bounds in three dimensions", *Extreme Mech. Lett.* **12** (2017), p. 97-100.

[78] J. Qu, M. Kadic, M. Wegener, "Poroelastic metamaterials with negative effective static compressibility", *Appl. Phys. Lett.* **110** (2017), no. 17, article no. 171901.

[79] J. Qu, M. Kadic, A. Naber, M. Wegener, "Micro-structured two-component 3D metamaterials with negative thermal-expansion coefficient from positive constituents", *Sci. Rep.* **7** (2017), p. 40643.